Journal of Manufacturing Engineering, December, 2016, Vol. 11, Issue. 4, pp 178-183

PREDICTING PITTING CORROSION RATE OF WELD NUGGET (STIR ZONE) OF FRICTION STIR WELDED DISSIMILAR JOINTS OF ALUMINIUM – MAGNESIUM ALLOYS

***R.Kamal Jayaraj[1], S. Malarvizhi[2] and V.Balasubramanian[3]**

[*1]Research Scholar, [2]Associate Professor and [3]Professor, Centre for Materials Joining and Research (CEMAJOR), Department of Manufacturing Engineering, Annamalai University, Annamalai Nagar – 608 002, Tamil Nadu, India.

ABSTRACT

Joining of Magnesium (Mg) and Aluminium (Al) alloys by fusion welding processes is very difficult due to formation of intermetallic compounds in weld metal. This problem could be overcome by friction stir welding (FSW) because of solid state welding conditions. However, Al/Mg dissimilar FSW joints are more prone to corrosion attack due to the formation of intercalated microstructure in weld nugget (stir zone). The limitation of low corrosion resistance restricts practical applications of these types of joints. In this investigation, an attempt has been made to develop an empirical relationship to predict the pitting corrosion rate of nugget region of friction stir welded dissimilar joints of AA6061 Al – AZ31B Mg alloys. Three important corrosion test parameters, namely, chloride ion concentration, pH value and exposure time are chosen as input parameters. Three factors, five level, central composite rotatable design matrix is used to minimize the number of experimental conditions. Response surface methodology is used to develop an empirical relationship. The developed relationship can be effectively used to predict the pitting corrosion rate of friction stir welded dissimilar joints of AA6061 Al – AZ31B Mg alloys at 95 % confidence level. The methodology adopted to develop the relationship is presented in this paper.

Key words: *Friction stir welding, Dissimilar joint, Aluminium alloy, Magnesium alloy, Pitting corrosion rate, Response surface methodology.*

1. Introduction

Magnesium (Mg) alloys are lightweight structural materials used for automotive, aerospace and ship building industries, due to low density and high specific strength [1, 2]. The ability to join Mg alloys to other engineering materials such as aluminum (Al) alloy would consent to further design flexibility and expand their applications. It is known that fusion welding between Al and Mg alloys cannot be practically used because of the formation of brittle intermetallic compounds at the weld zone [3–5]. To overcome this metallurgical problem, non-fusion welding process such as friction stir welding (FSW), friction welding (FW), diffusion bonding can be used to join these two alloys. FSW is a solid-state joining process, which was patented in the year 1991 by the Welding Institute in the United Kingdom [6]. This process comprises low residual stresses and reduced defects compared to the conventional fusion welding techniques [7, 8]. Presently, more attention has been given on FSW of dissimilar materials such as Al and Mg alloys to combine the benefits of two alloys [9–12].

Many researchers [13, 14] investigated the microstructural evolutions of dissimilar FSW joints of Al and Mg alloys. Simoncini and Forcellese [15] obtained sound dissimilar joints using the ‘‘pin’’ tool configuration. They found that an obvious improvement in the surface appearance and mechanical properties by placing aluminium alloy in the advancing side and magnesium alloy in the retreating side. Seetharaman et al. [16] investigated the corrosion behaviour of friction stir welded AA2024 aluminium alloy immersed in NaCl solution with different immersion times using immersion corrosion tests. It was resulted that with the increase of immersion time, the corrosion rate decreases for the specimens undergoing immersion corrosion tests. However, the corrosion behaviour of dissimilar FSW joints of Al and Mg alloys has been rarely studied. Hence in this investigation, an attempt has been made to predict the pitting corrosion rate of weld nugget region (stir zone) of dissimilar FSW joints of Al and Mg alloys by developing an empirical relationship incorporating, chloride ion concentration, pH value and immersing time.

**Corresponding Author - E- mail: jayaraj_kamal@yahoo.co.in*

Table 1. Chemical composition (wt. %) of AA6061 aluminium and AZ31B magnesium alloys

Alloy	Al	Zn	Si	Mn	Cu	Cr	Mg
AA6061	Bal	-	0.6	-	0.25	0.2	1.0
AZ31B	3.0	1.0	0.1	0.6	0.04	-	Bal

2. Experiment

2.1 Fabrication of joints and specimen preparation

A 6 mm thick rolled plates of AZ31B Mg alloy and AA6061-T6 Al alloy plates were used as base materials in this investigation. The chemical compositions of these alloys are listed in Table 1. To fabricate FSW joint, the plates were cut to the required size (150 mm x75 mm) by power hacksaw. A square butt joint was obtained by securing the plates in position using mechanical clamps. The welding direction was normal to the rolling direction of the plates. Fig. 1a shows the positioning of the plates during welding; AA6061 aluminium alloy is placed in the advancing side and AZ31B magnesium alloy in retreating side. Taper threaded cylindrical tool made of super high speed steel (Fig. 1b) was used to fabricate the joints.

A computer numerical controlled (CNC) friction stir welding machine (22 kW; 4000 rpm; 60 kN) was used to fabricate the joints. The FSW parameters were optimized by conducting a lot of welding trials. The welding conditions which produced defect free joints were taken as optimized welding conditions. The optimized welding parameters and tool dimensions are presented in Table 2. The optical micrograph of parent metals and stir zone of dissimilar friction stir welded joint are shown in Fig. 2.

From the fabricated joints, the specimens were extracted from weld nugget region of the FSW joints for conducting potentiodynamic polarisation test with the dimensions of 20 x 20 x 6 mm. The scheme of extraction of corrosion test samples is shown in Fig.1c. Before corrosion test, the specimens were grounded and polished with 600 to 1500 grit SiC paper. Finally, it was cleaned with acetone and washed in distilled water and then dried by warm flowing air. The photograph of the polished corrosion test specimen is shown in Fig. 1d. The photograph of the sample placed in a pitting corrosion test cell (Fig. 1e). The Gill-AC potentiostat instrument was used to conduct the potentiodynamic polarization test in NaCl solution at different conditions as shown in Fig. 1f.

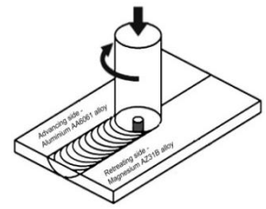

a. FSW of dissimilar joint (Schematic diagram)

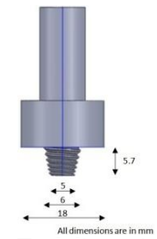

b. Tool dimensions

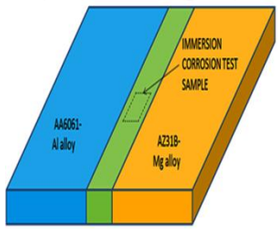

c. Specimen extraction scheme

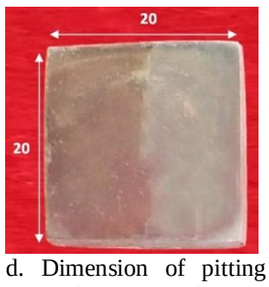

d. Dimension of pitting corrosion test specimen

e. Pitting corrosion test cell

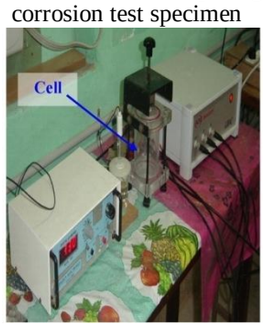

f. Gill AC Potentiostat

Fig.1 Experimental details

2.2 Selection of experimental design matrix

A central composite rotatable three-factor, five level factorial design matrix was selected to minimize number of experiments. The experimental design matrix consisting 20 sets of coded conditions, comprising a full replication three-factor factorial design of eight points, six star points, and six center points was used. Table 3 presents the range of factors considered and Table 4 shows the 20 sets of actual values and output responses of the experiments. The lower and upper limits of the parameters were coded as -1.682 and +1.682, respectively. Thus, the 20 experimental runs allowed for the estimation of the linear, quadratic, and two-way interactive effects of the variables. The way of designing such a matrix is dealt with elsewhere [17, 18]. The coded values for

intermediate levels can be calculated from the relationship.

$$X_i = \frac{1.682[2X - (X_{max} + X_{min})]}{X_{max} - X_{min}} \cdots\cdots\cdots\cdots\cdots\cdots (1)$$

Where X_i is the required coded value of a variable X and X is any value of the variable from X_{min} to X_{max}; X_{min} is the lower level of the variable; X_{max} is the upper level of the variable.

2.3 Pitting corrosion rate evaluation

NaCl solutions with concentrations of 0.2, 0.36, 0.6, 0.84 and 1 mol/L were prepared. The pH value was measured using a digital pH meter and varied from 3 to 11 as prescribed by design matrix. The corrosion rate of the weld nugget region was calculated from current density multiplied by a metal factor. The expression is followed as,

$$Corrosion\ rate, \frac{mm}{year} = \frac{Metal\ \ factor\ X\ i_{corr}}{1000} \cdots\cdots\cdots (2)$$

The current density (i_{corr}) is expressed as,

$$i_{corr}, A/m^2 = \frac{b_a X b_c}{2.3 X R_p X (b_a + b_c)} \cdots\cdots\cdots (3)$$

Where, b_a is anodic tafel slope in volts, b_c is the cathodic tafel slope in volts and R_p is the polarization resistance in Ω/m^2.
Metal factor is calculated from,

$$Metal\ \ factor = \frac{t\ X\ K}{\rho} \cdots\cdots\cdots (4)$$

Where 't' is the seconds in year, 'ρ' is the density in g/cm^2 and 'K' is the electrochemical equivalent in g/coulombs. From equation (2) the pitting corrosion rates were calculated and the results were tabulated in Table. 4.

Table 2. Optimized welding conditions and process parameters used to fabricate the dissimilar joints.

Tool rotational speed (rpm)	Tool travel speed (mm/min)	Axial force (kN)	Tool shoulder diameter (mm)	Tool pin diameter (mm)
600	30	14	18	5-6

Table 3. Important factors and their levels

Si. No.	Factor	Levels				
		-1.68	-1	0	+1	+1.68
1	Chloride ion con. (Mol)	0.2	0.36	0.6	0.84	1
2	pH value	3	4.62	7	9.38	11
3	Exposure time (mins)	5	15	30	45	55

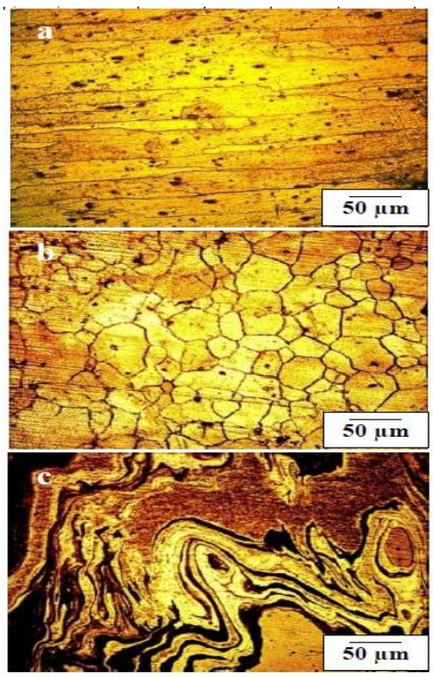

Fig 2. Optical micrograph of (a) AA6061 aluminium (b) AZ31B magnesium alloy and (c) weld nugget region of friction stir welded dissimilar joints.

3. Developing an empirical relationship

A second order quadratic model was developed to correlate the pitting corrosion test parameters. The response (corrosion rate) is a function of chloride ion concentration (C), pH value (P), and exposure time (T).

$$Pitting\ corrosion\ rate = f\{C, P, T\} - - - - - (5)$$

The equation should contain main and interaction effects of all variables and hence the response is expressed as

$$Y = b_o + \sum b_i x_i + \sum b_{ii} x_i^2 + \sum b_{ij} x_i x_j \cdots\cdots\cdots (6)$$

For three factors, the selected response could be expressed as

$$PCR = b_0 + b_1(C) + b_2(P) + b_3(T) + b_{12}(CP) + b_{13}(CT) + b_{23}(PT) + b_{11}(C^2) + b_{22}(P^2) + b_{33}(T^2) \cdots\cdots (7)$$

Where, b_0 is the average of responses (corrosion rate) and b_1, b_2, b_3,…,b_{11}, b_{12}, b_{13},…,b_{22},

b_{23}, b_{33} are the coefficients that depend on their respective main and interaction factors, which were calculated using the expression given below,

$$B_i = \sum (X_i, Y_i) / n \cdots\cdots\cdots (8)$$

where 'i' varies from 1 to n, in which X_i is the corresponding coded value of a factor and Y_i is the corresponding response output value (corrosion rate) attained from the experiment and 'n' is the total number of combination considered. All the coefficients were calculated by applying central composite face centred design using the Design Expert statistical software package. After determining the significant coefficients (at 95 % confidence level), the final relationship was developed by using these coefficients.

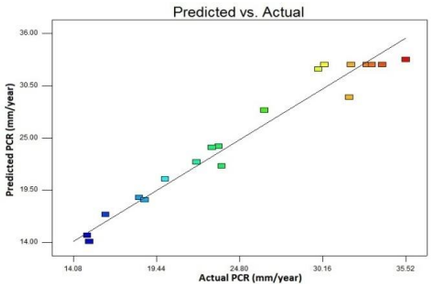

Fig. 3 Correlation graph

Table 4. Design matrix and experimental results.

Exp. No.	Actual values			Output responses	
	Con. (C)	pH (P)	Time (T)	I_{corr} (mA/cm²)	CR (mm/year)
1	0.36	4.62	15	1.16	18.33
2	0.84	4.62	15	1.49	23.46
3	0.36	9.38	15	1.68	26.39
4	0.84	9.38	15	1.90	29.88
5	0.36	4.62	45	0.96	15.11
6	0.84	4.62	45	1.19	18.68
7	0.36	9.38	45	1.27	19.99
8	0.84	9.38	45	1.46	23.02
9	0.20	7.00	30	0.95	14.98
10	1.00	7.00	30	1.50	23.65
11	0.60	3.00	30	1.03	16.16
12	0.60	11.00	30	2.02	31.87
13	0.60	7.00	5	2.26	35.52
14	0.60	7.00	55	1.40	22.02
15	0.60	7.00	30	2.12	33.32
16	0.60	7.00	30	2.10	32.99
17	0.60	7.00	30	1.92	30.27

The final empirical relationship derived by the above method to estimate the corrosion rate of nugget region (stir zone) of friction stir welded Al/Mg dissimilar joint is given below,

$$PCR\left(\frac{mm}{year}\right) = -53.03 + 122.12(C) + 10.81(P) + 0.42(T) - 0.48(CP) - 0.07(CT) - 0.02(PT) - 89.52(C^2) - 0.60(P^2) - 0.007(T^2) \cdots\cdots (9)$$

To find the significant main and interaction factors the analysis of variance (ANOVA) technique was used. Table 5 shows the ANOVA results for second order response surface model. The determination coefficient (r^2) indicated the goodness of fit for the model. The model F-value of 28.48 implies the model is significant. There is only a 0.01% chance that a "Model F-Value" this large could occur due to noise. Values of "Prob > F" less than 0.0500 indicate model terms are significant. In this case C, P, T, C^2, P^2, T^2 are significant model terms.

Values greater than 0.1000 indicate the model terms are not significant. If there are many insignificant model terms (not counting those required to support hierarchy), model reduction may improve your model. The "Lack of Fit F-value" of 2.92 implies the lack of fit is not significant relative to the pure error. There is a 13.24% chance that a "Lack of Fit F-value" this large could occur due to noise. Non-significant lack of fit is good. The "Pred R-Squared" of 0.7740 is in reasonable agreement with the "Adj R-Squared" of 0.9287. "Adeq Precision" measures the signal to noise ratio, a ratio greater than 4 is desirable. Ratio of 14.466 indicates an adequate signal. Each observed value is compared with the predicted value calculated from the model is shown in the Fig. 3.

Table 5. ANOVA test results

Source	Sum of square	Mean square	F value	p-value Prob> F	
Model	900.59	100.06	28.48	< 0.0001	significant
C	65.06	65.06	18.52	0.0016	
P	184.02	184.01	52.37	< 0.0001	
T	141.62	141.62	40.31	< 0.0001	
CP	0.59	0.5989	0.17	0.6884	
CT	0.50	0.5065	0.14	0.7121	
PT	3.47	3.4702	0.99	0.3437	
C^2	369.53	369.53	105.2	< 0.0001	
P^2	166.84	166.83	47.48	< 0.0001	
T^2	42.64	42.639	12.14	0.0059	
Residual	35.14	3.5135			
Lack of Fit	26.17	5.2337	2.92	0.1324	not significant
Pure Error	8.97	1.7934			
Cor Total	935.72				

To validate the developed relationship, three confirmation experiments were conducted by varying the concentration of chloride ion, pH and exposure time; the values were chosen randomly within the range of test parameters presented in Table 3.

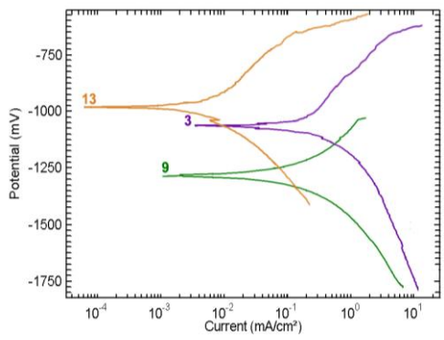

Fig. 4 Potentiodynamic polarization curves for Al/Mg FSW dissimilar joints of WZ tested in different conditions of NaCl solution.

Table 6. Validation test results

Sl. No	C (Mol)	P	T (mins)	Actual CR (mm/ year)	Predicted CR (mm/year)	Variation (%)
1	0.4	5	6	20.14	21.08	-0.94
2	0.5	4	11	21.26	20.84	0.42
3	0.9	9	7	29.58	30.06	-0.48

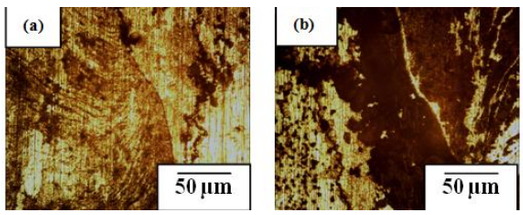

Fig. 5 Optical micrograph of the corrosion test specimens (a) Minimum corrosion attack (b) Maximum corrosion attack

The actual response was calculated from the average of three measured results. Table 6 summarizes the experimental values, predicted values and the variation. The validation results revealed that the developed empirical relationship is quite accurate as the variation is ±1 %.

The potentiodynamic polarization test was performed to evaluate to the corrosion behavior of weld nugget of friction stir welded dissimilar joints of aluminium – magnesium alloys in different solutions. From the 20 experiments, only 3 curves (low, medium and high corrosion rates) were showed in Fig. 4. From this polarization curve current density (i_{corr}) and corrosion potential (E_{corr}) were noted as shown in table 4. The corrosion rate dependent on corrosion current density when the i_{corr} increases the corrosion rate also increases.

Fig.5. reveals the optical micrograph of the corrosion test samples which exhibited minimum and maximum corrosion rates. In Fig (5a & 5b), severe corrosion attack was observed in magnesium alloy. The potential difference between Al and Mg in their galvanic couple can accelerate the initiation of pitting corrosion of Mg. The material with a lower free corrosion potential in the galvanic couple acts as anode and corrodes preferentially [19], but the rate of the galvanic corrosion is determined not only by the potential differences but also much more by polarization resistance [20]. Al alloy consists of thin oxide film will possesses remarkable corrosion resistance [21]. Therefore, in Al/Mg galvanic couple, Mg acts as anode while Al acts as cathode. For the galvanic couple, since the cathode side (Al) has a higher corrosion resistance compared with anodic side (Mg). In this, the maximum and minimum corrosion rate was observed in (0.60 mol/L chloride ion concentration, 7 pH and 5 hr exposure time) and (0.20 mol/L chloride ion concentration, 7 pH and 30 mins exposure time), respectively. At this point in both the condition pH remain constant but the chloride ion concentration and exposure time may vary. The higher amount of chloride ion concentration and long duration of exposure results the higher corrosion attack [22, 23].

4. Conclusion

- An empirical relationship has been developed to predict the pitting corrosion rate of weld nugget region of friction stir welded dissimilar joints of AA6061 Al – AZ31B Mg alloys incorporating important corrosion test parameters. The developed relationship can be effectively used to estimate the pitting corrosion rate of weld nugget region of friction stir welded dissimilar joints of AA6061 Al – AZ31B Mg alloys at 95 % confidence level.
- The highest corrosion rate of 35.52 mm/year is observed under the test conditions of 0.60 mol/L chloride ion concentration, 7 pH and 5 hr exposure time. The lowest corrosion rate of 14.98 mm/year is observed under the test

condition of 0.20 mol/L chloride ion concentration, 7 pH and 30 mins exposure time.

- Of the three corrosion test parameters, pH value of the solution is found to be more aggressive parameter followed by chloride ion concentration and exposure time as per 'F' values.

Acknowledgements

The authors wish to express their sincere thanks to Council of Scientific and Industrial Research (CSIR), New Delhi for the financial support to carry out this investigation through sponsored project No. 22(0615)/13/EMR-II dated 26.02.2013.

References

1. *Ebert T and Mordike B L (2001), "Magnesium: Properties-applications-potential", Material Science and Engineering A, Vol. 302(1), 37–45.*
2. *Agnew S R Mehrotra P Lillo T M Stoica G M and Liaw P K (2005), "Texture evolution of five wrought magnesium alloys during route A equal channel angular extrusion: Experiments and simulations", Acta Materialia, Vol. 53(11), 3135–3146.*
3. *Lee W B Yeon Y M and June S B (2003), "The mechanical properties related to the dominant microstructure in the weld zone of dissimilar formed Al joints by friction stir welding", Journal of Material Science, Vol.38, 4183–91.*
4. *Paglia C S and Buchheit R G (2006), "Microstructure, microchemistry and environmental cracking susceptibility of friction stir welded 2219-T87", Material Science and Engineering A, Vol. 429, 107–14.*
5. *Chang W S Kim H J Noh J S and Bang H S (2006), "The evaluation of weld ability for AZ31B-H24 and AZ91C-F Mg alloys in friction stir", Key Engineering Materials, Vol. 321–323II, 1723–8.*
6. *Thomas W M Nicholas E D Needham J C Murch M G Temple smith P and Dawes C J (1991), "International Patent Application", PCT/GB92/02203.*
7. *Paglia C S Carroll M C Pitts B C Reynolds T and Buchheit R G (2002), "Strength, corrosion and environmentally assisted cracking of a 7075-T6 friction stir weld", Materials Science Forum, Vol. 396–402, 1677–1684.*
8. *Zettler R Silva A A M Rodrigues S Blanco A and Santos J F (2006), "Dissimilar Al to Mg alloy friction stir weld", Advance Engineering Materials, Vol. 8, 415–21.*
9. *McLean A A Powell G L F Brown I H and Linton V M (2003), "Friction stir welding of magnesium Alloy AZ31B to aluminum alloy 5083", Science and Technology of Welding and Joining, Vol. 8, 462–4.*
10. *Shiqematsu I Kwon Y J Suzuki K Imai T and Saito N (2003), "Joining of 5083 and 6061Aluminum Alloys by friction stir welding", Materials Science Letters, Vol. 22, 353–6.*
11. *Sato Y S Park S H C Michiuchi M and Kokawa H (2004), "Constitutional liquation during dissimilar friction stir welding of Al and Mg alloys", Scripta Materialia, Vol. 50, 1233–6.*
12. *Somasekharan A C Murr L E (2004), "Microstructures in friction-stir welded dissimilar magnesium alloys and magnesium alloys to 6061-T6 aluminum alloy", Materials Characterization, Vol. 52, 49–64.*
13. *Kostka A Coelho R S Dos Santo J and Pyzalla A R (2009), "Microstructure of friction stir welding of aluminium alloy to magnesium alloy", Scripta Materialia, Vol. 60, 953–956.*
14. *Somasekharan A C and Murr L E (2004), "Microstructures in friction-stir welded dissimilar magnesium alloys and magnesium alloys to 6061-T6 aluminum alloy", Materials Characterization, Vol. 52, 49– 64.*
15. *Simoncini M and Forcellese A (2012), "Effect of the welding parameters and tool configuration on micro- and macro-mechanical properties of similar and dissimilar FSWed joints in AA5754 and AZ31 thin sheets", Materials and Design, Vol. 41, 50–60.*
16. *Seetharaman R Ravisankar V and Balasubramanian V (2014), "Effect of immersion time on the corrosion behavior of friction stir welded AA2024 aluminium alloy welds", Journal of Manufacturing Engineering, Vol. 9(3), 143-148.*
17. *Khuri A I and Cornell J A (1996), "Response Surfaces", Design and Analysis, New York, Marcel Dekker Ltd., 405.*
18. *Miller R G Freund J E and Johnson D E (1999), "Probability and Statistics for Engineers", New Delhi, Prentice of Hall of India Pvt Ltd., 658.*
19. *Deshpande K B (2010), "Validated numerical modeling of galvanic corrosion for couples: Magnesium alloy (AE44)–mild steel and AE44–aluminium alloy (AA6063) in brine solution", Corrosion Science, Vol.52 (10), 3514-3522.*
20. *El-Dahshan M E Shams El Din A M Haggag H H (2002), "Galvanic corrosion in the systems titanium/316L stainless steel/Al copper in Arabian water", Desalination, Vol.142(2), 161-169.*
21. *Szklarska-Smialowska Z (1999), "Pitting corrosion of aluminum", Corrosion Science, Vol. 41, 1743-1767.*
22. *Hikmet Altun and Sadri Sen (2004), "Studies on the influence of chloride ion concentration and pH on the corrosion and electrochemical behaviour of AZ63 magnesium alloy", Materials and Design, Vol.25, 637–643.*
23. *Song G Johannesson B Hapugoda S and StJohn D (2004), "Galvanic corrosion of magnesium alloy AZ91D in contact with an aluminum alloy, steel and zinc", Corrosion Science, Vol.46, 955–977.*

Nomenclature

Symbol	Meaning	Unit
C	Chloride ion concentration	Mols
P	pH	-
T	Time	mins
CR	Corrosion rate	mm/year
I_{corr}	Corrosion current density	mA/cm²
E_{corr}	Corrosion potential	mV_{SCE}

